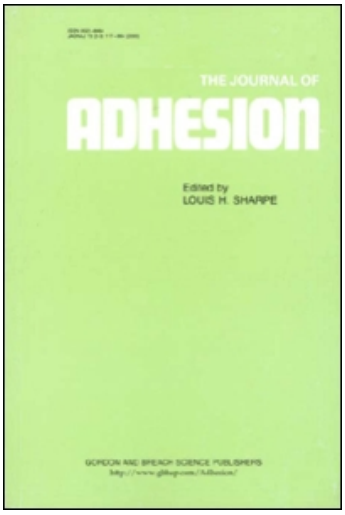

The Journal of Adhesion
Publication details, including instructions for authors and subscription information:
http://www.informaworld.com/smpp/title~content=t713453635

CALCULATION OF VAN DER WAALS FORCES WITH DIFFUSE COATINGS: APPLICATIONS TO ROUGHNESS AND ADSORBED POLYMERS

Raymond R. Dagastine[a]; Michael Bevan[a]; Lee R. White[a]; Dennis C. Prieve[a]
[a] Center for Complex Fluid Engineering and Department of Chemical Engineering, Carnegie Mellon University, Pittsburgh, Pennsylvania, USA

Online publication date: 10 August 2010

To cite this Article Dagastine, Raymond R. , Bevan, Michael , White, Lee R. and Prieve, Dennis C.(2004) 'CALCULATION OF VAN DER WAALS FORCES WITH DIFFUSE COATINGS: APPLICATIONS TO ROUGHNESS AND ADSORBED POLYMERS', The Journal of Adhesion, 80: 5, 365 — 394
To link to this Article: DOI: 10.1080/00218460490465696
URL: http://dx.doi.org/10.1080/00218460490465696

The Journal of Adhesion, 80: 365–394, 2004

ISSN: 0021-8464 print/1545-5823 online
DOI: 10.1080/00218460490465696

Taylor & Francis
Taylor & Francis Group

CALCULATION OF VAN DER WAALS FORCES WITH DIFFUSE COATINGS: APPLICATIONS TO ROUGHNESS AND ADSORBED POLYMERS

Raymond R. Dagastine
Michael Bevan
Lee R. White
Dennis C. Prieve
Center for Complex Fluid Engineering and Department of Chemical Engineering, Carnegie Mellon University, Pittsburgh, Pennsylvania, USA

A novel method using Lifshitz continuum theory to account for the effects of surface roughness was developed. The method treats roughness as a diffuse film whose dielectric properties vary continuously between those of the substrate and those of the solvent: AFM measurements of surface topography are used to deduce the volume-fraction profile of substrate in solvent which in turn is converted into a dielectric-permittivity profile using the Clausius-Mossoti equation as a mixing rule. Calculations show orders of magnitude of reduction in the van der Waals force between rough surfaces at contact compared with smooth surfaces, with the amount of reduction dependent on the shape of the volume-fraction profile as well as the total depth of the roughness. These predictions help account for discrepancies observed previously between the Total Internal Reflection Microscopy (TIRM) data and calculations for smooth polystyrene surfaces in water, with or without physisorbed polymer, without introducing any adjustable parameters.

Keywords: Roughness; van der Waals forces; Lifshitz theory; Adsorbed polymers

Received 9 September 2003; in final form 11 March 2004.

One of a collection of papers honoring Jacob Israelachvili, the recipient in February 2003 of *The Adhesion Society Award for Excellence in Adhesion Science, Sponsored by 3M*.

Current address of Raymond R. Dagastine: School of Chemistry, University of Melbourne, Parkville, Victoria 3010, Australia.

Current address of Michael Bevan: Dept. of Chemical Engineering, Texas A & M University, College Station, TX 77845.

Address correspondence to Dennis C. Prieve, Center for Complex Fluids and Department of Chemical Engineering, Carnegie Mellon University, Pittsburgh, PA 15213-3890, USA. E-mail: dcprieve@cmu.edu

INTRODUCTION

Deviations between experimental measurements of colloidal forces and theoretical predictions are commonly attributed to surface roughness [1, 2]. The mediation of colloidal forces by surface roughness also is being exploited to tailor dispersion properties (*e.g.*, nanospheres are adsorbed to larger particles to control the amount and type of roughness in colloidal dispersions) [3]. The van der Waals force is ubiquitous in colloidal dispersions; between like materials, it is always attractive and therefore the most common cause of dispersion destabilization. The significant impact of van der Waals forces on dispersion stability motivates the development of a method described below to account for the effects of surface roughness in the modern theoretical description of van der Waals forces. The strength of adhesion between surfaces in contact is also strongly dependent on van der Waals forces and can be affected by roughness.

In its most common form, intermolecular van der Waals attraction originates from the correlation that arises between the instantaneous dipole moment of any atom and the dipole moment induced in neighboring atoms. The earliest quantitative theory to describe van der Waals forces between two colloidal particles, each containing a statistically large number of atoms, was developed by Hamaker, who used pairwise summation of the atom−atom interactions. This approach neglects the multibody interactions inherent in the interaction of condensed phases. The modern theory for predicting van der Waals forces in continua was developed by Lifshitz, who used quantum electrodynamics [4, 5] to account for the many body molecular interactions and retardation within and between materials. Retardation is a reduction of the interaction because of a phase lag between the induced dipole response and instantaneous dipole that caused it; retardation generally increases with distance between the two dipoles.

In the Lifshitz theory, the magnitude of the nonretarded van der Waals force is proportional to the product of normalized differences in the dielectric permittivity $\varepsilon(\omega)$ between either of the two interacting materials (Figure 1, parts 1 and 2) and that of the intervening medium (Figure 1, part 3), where (at least for the nonretarded case)

$$\Delta_{jk} = \frac{\varepsilon_j - \varepsilon_k}{\varepsilon_j + \varepsilon_k}, \tag{1}$$

and j and k denote the materials (1, 2, or 3 as shown in Figure 1). The product $\Delta_{13}\Delta_{23}$ of the differences needs to be evaluated over the full spectrum of frequencies, which requires extensive spectroscopic characterization of all the materials. Due to absorption, the dielectric

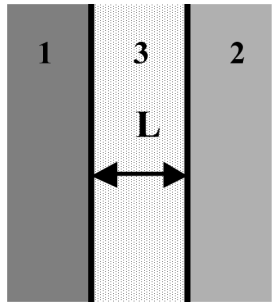

FIGURE 1 Two smooth half spaces, 1 and 2, separated by an intervening medium, 3.

function $\varepsilon(\omega)$ takes on complex values for real frequencies and is a highly nonmonotonic function of frequency. Using the mathematical principle of analytic continuation, this complicated function of real frequency, ω, can be mapped into a monotonically decreasing and purely real function of imaginary frequency, $i\xi$. Lifshitz theory was not widely used until Ninham and Parsegian [6] and others [7–9] developed a general model for the dielectric function whose parameters could be deduced from available absorption spectra by fitting to a set of damped harmonic oscillators. But even with as many as 18 adjustable parameters in the model, the dielectric spectra of water cannot be fitted exactly. We recently suggested a new iterative approach to obtaining the full dielectric spectra from available data without curve fitting [10, 11] and incorporated more recent spectroscopic data from inelastic X-ray scattering [12] for water.

In this manuscript we present a new method to incorporate surface roughness into Lifshitz continuum theory of van der Waals forces. The rough interface between two adjacent media is treated as a diffuse region whose dielectric properties vary continuously between those of the substrate and those of the fluid outside. In the calculations, we discretize the diffuse region into a series of thin uniform coatings. The dielectric properties of each coating are based on the volume fraction in that slice, as suggested by Figure 2. Modifications to Lifshitz theory for the interaction between half spaces coated with multiple layers has been previously described [13]. The only new information required is the volume-fraction profile in the rough interface, which can be obtained *via* standard topography measurement techniques, *e.g.*, scanning electron microscopy (SEM) or atomic force microscopy (AFM). This same approach is also used to calculate the interaction between halfspaces bearing physisorbed or chemisorbed polymer layers.

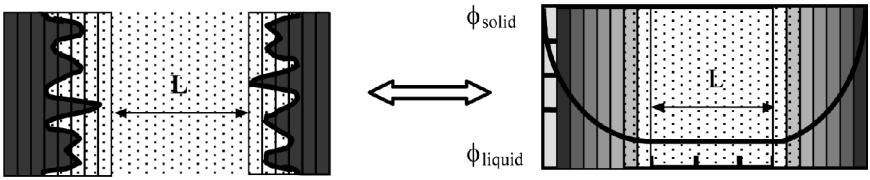

FIGURE 2 The two-dimensional cross section of two rough solid interfaces separated by a liquid is on the left. The two-dimensional cross section on the right is the result of smoothing the surface roughness laterally (parallel with the smooth interfaces), converting the rough interfaces to a series of homogenous coatings with volume fraction, ϕ, varying from solid to liquid.

THEORY

Previous Attempts to Model Surface Roughness

There have been a number of approaches employed to account for the effects of roughness on van der Waals forces using the linear superposition approximation. The Hamaker approach employs integrals over macroscopic volumes, which is conducive to simple geometries such as spherical or conical asperities on flat surfaces [14, 15] and even more complicated geometries [16]. A number of such integrations have been employed, which are well summarized in [16–18], but there has been far less work on taking surface roughness into account using continuum theory.

An analytic expression for the nonretarded van der Waals interaction for two parallel rough surfaces was developed by Mazur and Maradudin [19, 20]. They employed the approach developed by van Kampen *et al.* [21], which determines the dispersion relation for the nonretarded van der Waals force by determining the nonzero surface modes for propagation of a time-dependent electromagnetic field at the interface of two surfaces. For two flat surfaces separated by a third medium, the nonzero surface modes are determined by solving Laplace's equation for potential, assuming continuity of potential and normal displacement at the interfaces. The geometry of an arbitrarily rough surface makes applying these boundary conditions more difficult than for a flat interface. Mazur and Maradudin treat roughness as a stochastic process, such that the boundary conditions are ensemble averages over a stochastic number of surfaces. They then solve the dispersion relation analytically in the limit where the ratio of the surface separation to transverse spacing (of surface features) is large. The results of [19, 20] also are limited because a vacuum

separates the two surfaces and a Gaussian distribution of roughness was used.

Czarnecki and Dabros [22] developed a semiempirical correction factor to account for surface roughness between parallel half spaces. Their correction factor was developed by using a pairwise summation of the intermolecular interactions with a Gaussian distribution for roughness. The correction requires the peak-to-valley height of the roughness. The interaction between rough half-spaces was extended to spheres using a geometric correction factor [23]. Although the approach of Czarnecki employs pairwise summation methods and Mazur and Maradudin [19, 20] apply a continuum theory, there is a notable correlation between the two studies. They both conclude that, to leading order, surface roughness can be accounted for by moving the boundary of the two interfaces further apart by a distance dependent on the overall height of the surface roughness.

Bevan and Prieve [2] compared experimental measurements of retarded van der Waals forces between two polystyrene surfaces (PS) in water with Lifshitz theory for smooth surfaces and found that the theory overpredicts the retarded attraction, despite having the full dielectric spectra for the materials. Treating roughness as a *homogeneous* film with dielectric properties midway between PS and water gave slightly better agreement with experiments, but the functional form for the separation dependence was not reproduced, regardless of what weighting factor was used to average the properties of PS and water. They suggested that a better model for roughness might be a *diffuse* film whose properties vary between those of PS and water. They obtained better agreement by using Czarnecki's semiempirical model of roughness.

Several studies of the effects on nonretarded van der Waals forces between macroscopic bodies with films of inhomogeneous dielectric properties have been made. Parsegian and Weiss [24] derived the nonretarded expression for two identical half spaces bearing a coating with inhomogeneous dielectric properties as a model for adsorbed polymer layers (earlier treatment using a Hamaker approach was done by Vold [25]). The dielectric properties smoothly varied with distance from those of the half space to those of the intervening medium. Weiss and coworkers [26] derived a more general result in order to vary the functional form of dielectric inhomogeneity in the coating, showing that for some cases the functional form had a significant effect on the van der Waals interaction. Kiefer and coworkers [27] derived an analogous expression for the nonretarded interaction between two spheres as well.

Lifshitz Theory for Halfspaces

Hamaker's linear superposition theory provides a single parameter (the Hamaker constant) to describe the interaction between macroscopic bodies. The interaction energy per unit area, E_{132}, between two half spaces of media 1 and 2, separated by medium 3, is given by (as shown in Figure 1)

$$E_{132} = -\frac{A_{132}}{12\pi L^2}, \tag{2}$$

where A_{132} is the Hamaker constant and L is the separation distance. Lifshitz continuum theory, which includes the effects of many-bodied interactions and retardation, effectively causes the Hamaker constant to vary with separation distance. The Hamaker function $A_{132}(L)$ for two infinite half spaces separated by an intervening third medium is given by [28]

$$A_{132} = -\frac{3}{2}k_b T {\sum_{n=0}^{\infty}}' \int_{r_n}^{\infty} x \ln\left\{\left[1 - \Delta_{13}\Delta_{23}e^{-x}\right]\left[1 - \bar{\Delta}_{13}\bar{\Delta}_{23}e^{-x}\right]\right\} dx, \tag{3}$$

$$\Delta_{jk} = \frac{\varepsilon_j s_k - \varepsilon_k s_j}{\varepsilon_j s_k + \varepsilon_k s_j} \quad \bar{\Delta}_{jk} = \frac{s_k - s_j}{s_k + s_j} \quad s_k^2 = x^2 + \left(\frac{2\xi_n L}{c}\right)^2 (\varepsilon_k - \varepsilon_3)$$

$$r_n = \frac{2L\xi_n\sqrt{\varepsilon_3}}{c} \quad \xi_n = \frac{2\pi n k T_b}{\hbar} \quad \varepsilon_k = \varepsilon(i\xi_n),$$

where c is the speed of light in a vacuum, k_b is the Boltzmann constant, T is temperature, $\hbar$ is Planck's constant divided by 2π, and the ξ_n are the sampling frequencies of the dielectric function $\varepsilon_n(i\xi)$. The prime indicates that the first term in the summation has half weight. The presence of electrolyte in the intervening medium screens the $n = 0$ term (see Appendix A). The dielectric permittivity, $\varepsilon(\omega)$, evaluated at a real frequency, ω, has a real and imaginary part,

$$\varepsilon(\omega) = \varepsilon'(\omega) + i\varepsilon''(\omega), \tag{4}$$

denoted by $'$ and $''$, respectively.

Lifshitz Theory with Uniform Coatings

The van der Waals interaction for a single coating on two half spaces was derived by Ninham and Parsegian [29, 30] *via* the surface modal approach developed by van Kampen (and a similar result found by Langbein [31]). For two symmetric coated half spaces (see Figure 3),

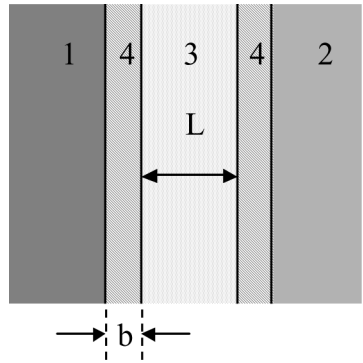

FIGURE 3 Two smooth half spaces with a symmetric homogeneous coating of material 4 with thickness b.

the Δ terms in Equation (3) become

$$\Delta_{31}(b) = \frac{\Delta_{34} + \Delta_{41} e^{-(bs_4/L)}}{1 + \Delta_{34}\Delta_{41} e^{-(bs_4/L)}}, \tag{5}$$

where b is the coating thickness and 4 is the coating material. The above expression is not restricted to identical coatings [32] on each half space: if half space 2 is instead coated with material 5, then Δ_{31} is still given by Equation (5), but Δ_{32} is given by an expression like Equation (5) except that 1 is replaced by 2, 4 is replaced by 5, and of course the layer thickness, b, is replaced by its appropriate symbol.

Equation (5) applies to a single coating layer (the case in Figure 3). If a second layer of thickness, h, of material 5 is added (see Figure 4),

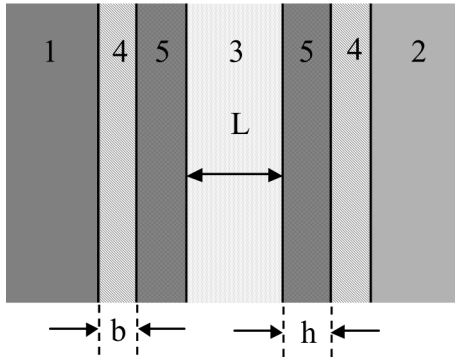

FIGURE 4 Two smooth half spaces with two symmetric homogeneous coatings of materials 4 and 5 with thickness b and h, respectively.

then Equation (5) becomes

$$\Delta_{31}(b,h) = \frac{\Delta_{35} + \Delta_{51}(b)e^{-(hs_5/L)}}{1 + \Delta_{35}\Delta_{51}(b)e^{-(hs_5/L)}}, \tag{6}$$

where Δ_{31} is now a function of Δ_{51}. The new Δ_{35} is defined according to Equation (3) and Δ_{51} is defined as in Equation (5):

$$\Delta_{51}(b) = \frac{\Delta_{54} + \Delta_{41}e^{-(bs_4/L)}}{1 + \Delta_{54}\Delta_{41}e^{-(bs_4/L)}}. \tag{7}$$

Combining Equations (6) and (7) leads to the rather complicated expression,

$$\Delta_{31}(b,h) = \frac{\Delta_{35} + \frac{\Delta_{54}+\Delta_{41}e^{-(bs_4/L)}}{1+\Delta_{54}\Delta_{41}e^{-(bs_4/L)}}e^{-(hs_5/L)}}{1 + \Delta_{35}\frac{\Delta_{54}+\Delta_{41}e^{-(bs_4/L)}}{1+\Delta_{54}\Delta_{41}e^{-(bs_4/L)}}e^{-(hs_5/L)}}\Delta_{c_N1}. \tag{8}$$

While the end results may appear convoluted, the general approach outlined above can be generalized for N coatings [13] (shown in Figure 5):

$$\Delta_{31}(c_1, c_2, \ldots, c_N) = \frac{\Delta_{3c_N} + \Delta_{c_N1}(c_1, c_2, \ldots, c_{N-1})e^{-(t_N s_N/L)}}{1 + \Delta_{3c_N}\Delta_{c_N1}(c_1, c_2, \ldots, c_{N-1})e^{-(t_N s_N/L)}}, \tag{9}$$

where c_i is the index for the coating material, t_i is the thickness and N is the number of coatings, where

$$\begin{aligned}\Delta_{c_N1}&(c_1, c_2, \ldots, c_{N-1}) \\ &= \frac{\Delta_{c_Nc_{N-1}} + \Delta_{c_{N-1}1}(c_1, c_2, \ldots, c_{N-2})e^{-(t_{N-1}s_{N-1}/L)}}{1 + \Delta_{c_Nc_{N-1}}\Delta_{c_{N-1}1}(c_1, c_2, \ldots, c_{N-2})e^{-(t_{N-1}s_{N-1}/L)}}\end{aligned} \tag{10}$$

and where Δ_{3c_N} and $\Delta_{c_Nc_{N-1}}$ above are defined using Equation (3).

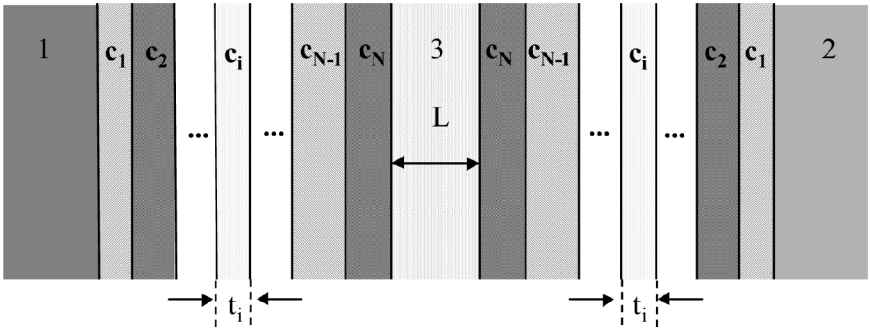

FIGURE 5 Two smooth half spaces with an arbitrary number, N, of homogeneous with coatings, c_i where i = 1...N, with a thickness t_i.

Diffuse Coatings as Multilayers

The rough interfacial region is divided into a series of layers (see Figure 2) such that each layer contains some of the substrate material and some of the intervening medium. The volume fraction of each phase is a function of distance from the substrate half space. Each layer is then treated as a homogenous coating with material properties that are intermediate between the two materials based on volume fraction. The volume fraction as a function of distance from the substrate is easily obtained from measurements of the surface topography. Using the surface topography obtained *via* AFM or SEM, a histogram of heights can be constructed and then integrated to compute the volume fraction as a function of height (*e.g.*, see Figure 6).

The mixing rule for the dielectric properties of each coating is based on that for solutions. The molecular polarizability of a pure substance α (a molecular property) is related to the dielectric permittivity (a continuum property) *via* the Lorentz-Lorenz formula* [34],

$$\frac{\varepsilon(\omega)-1}{\varepsilon(\omega)+2}=\frac{4\pi}{3}\rho\alpha, \tag{11}$$

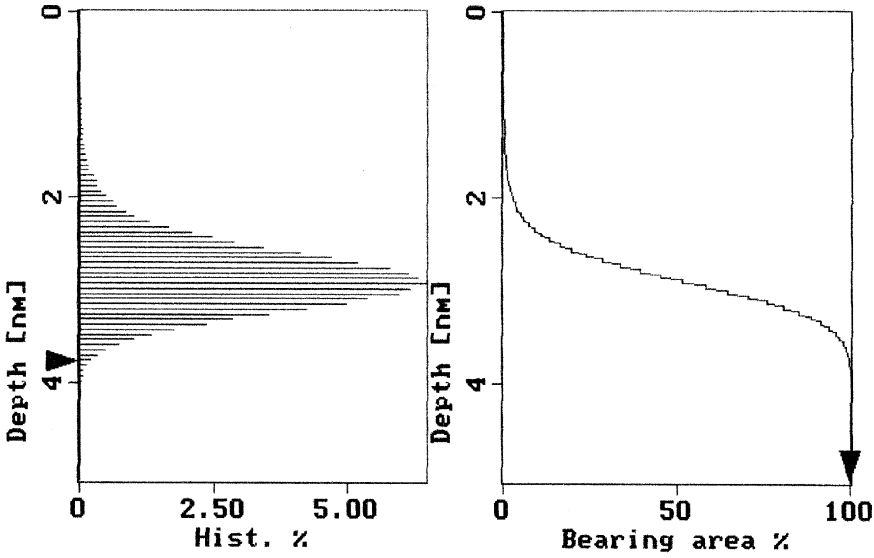

FIGURE 6 Bearing analysis for an AFM image (Figure 15) of a glass surface. The histogram of heights is integrated to produce the volume fraction of glass as a function of depth.

*Equation (11) has also been called the Clausius-Mossoti formula [33].

where ρ is the number density of molecules. If the molecules of a mixture are polarized to the same extent that they would be in a pure substance, then Equation (11) can be generalized for mixtures to [34]

$$\left(\frac{\varepsilon(\omega)-1}{\varepsilon(\omega)+2}\right)_{mixture} = \frac{4\pi}{3}\sum_i \rho_i \alpha_i, \tag{12}$$

where the sum is over the molecular species, i. Recognizing that the number density of a pure substance is $\rho = 1/v_m$, then (in the absence of any volume change on mixing) the number density of component i in a mixture can be written as $\rho_i = \phi_i/v_{mi}$, where ϕ_i is the volume fraction of material i. Using Equation (11) to eliminate v_{mi}, Equation (12) becomes

$$\left(\frac{\varepsilon(\omega)-1}{\varepsilon(\omega)+2}\right)_{mixture} = \sum_i \phi_i \left(\frac{\varepsilon(\omega)-1}{\varepsilon(\omega)+2}\right)_i. \tag{13}$$

While this mixing rule has been shown to work reasonably well for solutions like sulfuric acid and water [34], its suitability for dispersed phases of two immiscible components is less well established. In the limit in which the two phases are dispersed finely enough in one another so that the size of any given particle is very small compared with the wavelength, the mixture might be expected to obey the same mixing rule as a solution.

The above mixing rule is applicable for *electronic* polarization of a material, but the Lorentz-Lorenz formula does not apply at zero frequency because the predominant contribution to static dielectric constant of water arises from *orientational* polarization of permanent dipoles [35]. For zero frequency, an arithmetic mixing rule based on volume fraction is used:

$$\varepsilon(0)_{mixture} = \sum_{i=1}^{k} \phi_i \varepsilon_i(0), \tag{14}$$

where $\varepsilon_i(0)$ is the static dielectric constant for material i. Dielectric properties of each coating are determined from Equations (13) and (14), and then Equations (2) through (10) are used to calculate the Hamaker function and interaction energy.

RESULTS AND DISCUSSION

Uniform Coatings: Coating Properties versus Substrate Properties

Figure 7 shows the Hamaker function between two identical PS half-spaces coated by a film of tetradecane (TD) and separated by water

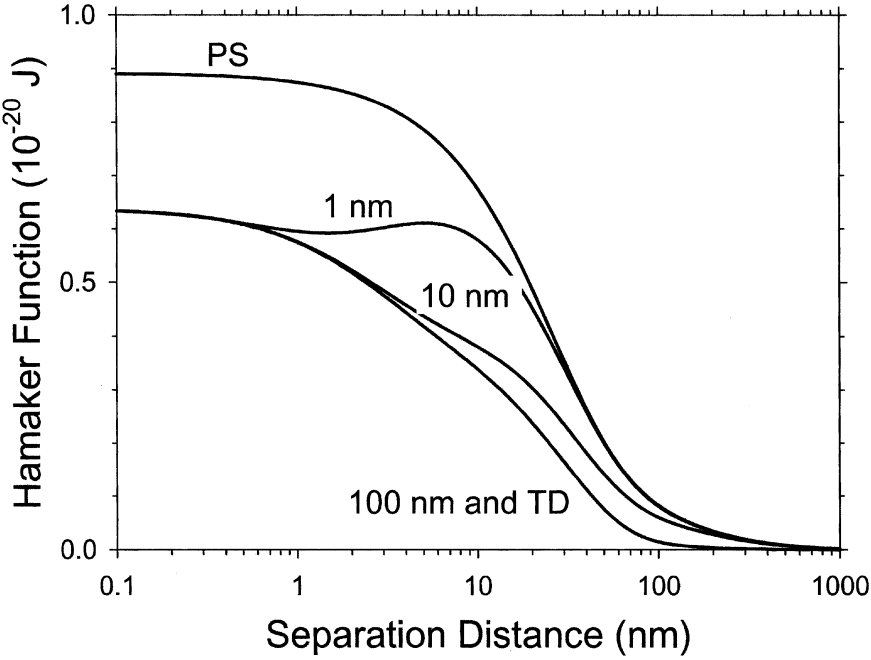

FIGURE 7 The Hamaker function for two PS half spaces separated by water with a coating of tetradecane (TD) with an increasing thickness (according to the schematic in Figure 3). The two limiting cases (two PS surfaces separated by water and two TD surfaces separated by water) bracket the coating results. Once the coating has reached 100 nm there is no visible difference between the coating and TD surface case.

containing 0.1 mM electrolyte. Also shown for comparison are the Hamaker functions between two uncoated PS halfspaces and two uncoated TD halfspaces. Notice that the Hamaker function for the coated halfspaces always tends toward that of the two uncoated TD halfspaces at small separations and tends toward that of the two uncoated PS halfspaces at large separations. Thus, the properties of the coating completely mask those of the substrate at small separations, whereas, the coating is completely invisible at large separations [28]. This conclusion will be important below when the interaction between rough surfaces is discussed.

At moderate separations, the Hamaker function for two coated halfspaces is a weighted average of that between two uncoated halfspaces of the substrate material and that between two uncoated halfspaces of the coating material, with the weighting factor for the coating

material decreasing monotically from unity at zero separation to zero at infinite separation. The weighting factor is approximately 0.5 at a separation distance equal to three times the coating thickness [28]. The conclusion, that the weighting factor depends on the ratio of the separation to the coating thickness, is also apparent in Equation (5), where the inverse of this ratio appears in the exponent.

Roughness as Diffuse Coating

A series of functional forms were employed to differentiate the effects of the distribution of material in the roughness layer. Different functional forms, which may be encountered in practice, were employed for the same overall roughness thickness. Either an exponential or ellipsoidal form were used (shown in Figure 8) with the linear decreasing function included for comparison. The ellipsoidal

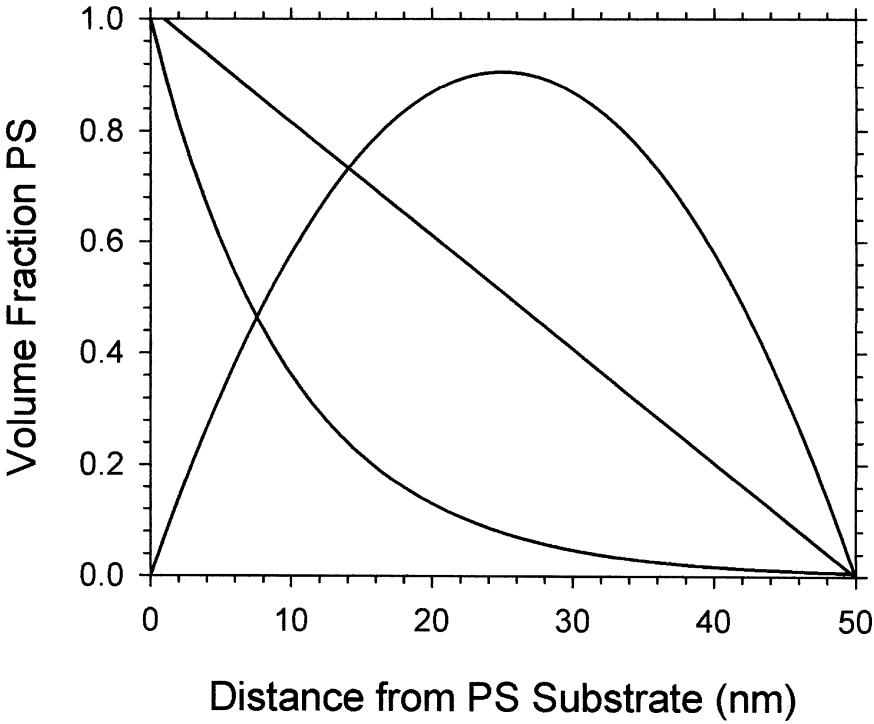

FIGURE 8 The volume fraction profiles for three different functional forms; linear, exponential decay, and for closed packed monolayer of spheres adsorbed to a smooth surface.

density function is the result of compiling the density function for a flat surface with a closed, packed monolayer of nanospheres adsorbed on the surface. The volume fraction for a monolayer of spheres as a function of surface depth is given by

$$\phi_{sphere} = \frac{3\pi(2ad - d^2)}{6\sqrt{3}a^2}, \tag{15}$$

where a is the radius of the sphere and d is the position ($0 \leq d \leq 2a$). This type of surface modification is one way to control surface roughness in colloidal dispersions.

The number of layers is increased until no visible effect is observed on the calculated Hamaker function. An example of this determination is shown in Figure 9, where the exponential volume fraction function (given in Figure 8) is used for two PS halfspaces separated by water.

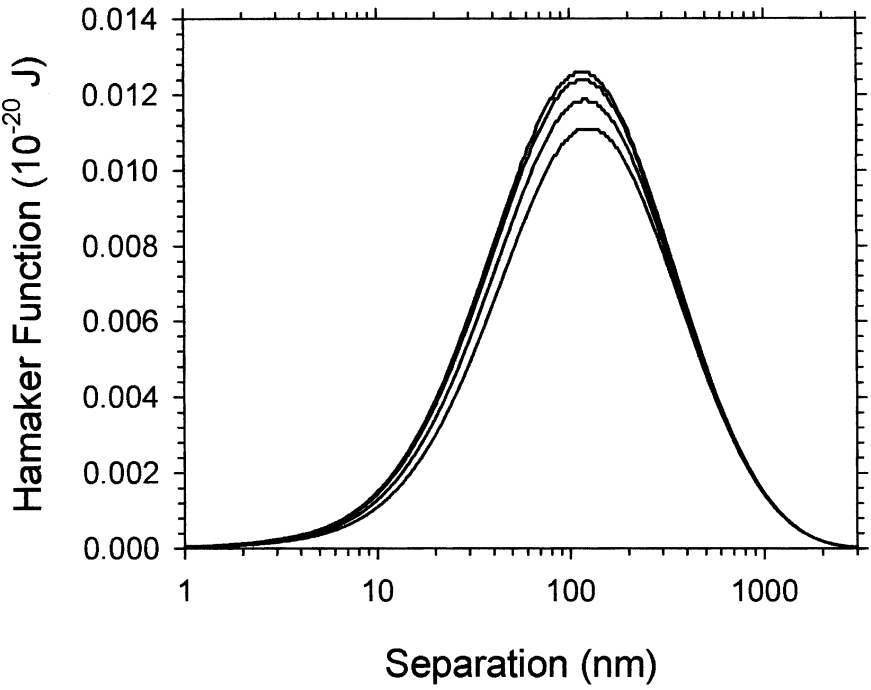

FIGURE 9 The Hamaker function for rough polystyrene surfaces separated by water in the presence of 0.1 mM binary electrolyte with an exponential volume fraction profile (from Figure 8) using the lateral smoothing procedure. The 50 nm diffuse region on either surface was discretized into 5, 10, 20, or 50 uniform layers (lower to upper curves).

The dielectric spectra for water and polystyrene were taken from Dagastine *et al.* [11] and Dagastine *et al.* [10], respectively. The volume fraction function must be sampled at a sufficient number of points to capture adequately the rate of change in volume fraction, and thus verification of adequate sampling may be required for volume fraction functions with large first derivatives. Increments of 1 nm (upper curve) appear to be adequate sampling for this calculation.

From the discussion of Figure 7 above, we recall that the Hamaker function at separations below three coating thicknesses is dominated by the properties of the outermost coating. If our discretized coating is to mimic a continuously varying coating, we expect that smaller thicknesses need to be chosen for the outer layers at smaller separations; in particular, the outer coating thickness must be small compared with separation distance to reflect the effect of the outer region of the diffuse film. The heuristic of 0.5–1 nm per coating is appropriate when the separation distance is greater than about 5 nm. At smaller separations we probably overestimate the strength of van der Waals attraction if the diffuse layer's properties tend toward those of the fluid separating the bodies. At separations below 5 nm, a more rigorous approach would be to neglect retardation effects and use the theory of Parsegian and Weiss [24].

Effect of Volume Fraction Distribution

In Figure 10 we compare the Hamaker functions calculated for rough surfaces using various volume fraction profiles illustrated in Figure 8. The effect of shape is evident, where the exponential decay has the weakest interaction (low-volume fraction of PS near the outer edge), and all three cases of surface roughness are significantly lower than for smooth half spaces. It is interesting to note that, at any given separation, the Hamaker function increases with the average PS volume fraction for the diffuse coating: the average volume fractions of PS in each diffuse coating are 69.7, 50, and 19.5% for the spherical, linear, and exponential profiles, respectively.

Figure 11 attempts to isolate the effect of changes in shape while keeping the thickness and the average volume fraction constant. The three shapes explored are a linear increase, a linear decrease, and a constant volume fraction with depth from the surface. All three layers have a average volume fraction of 50%. For any given separation distance, coatings having less PS near the outer edge lead to weaker attraction. Moreover, the differences between the three coatings become greater as the separation distance gets smaller. The reason is simple: the apparent dielectric properties of the coated

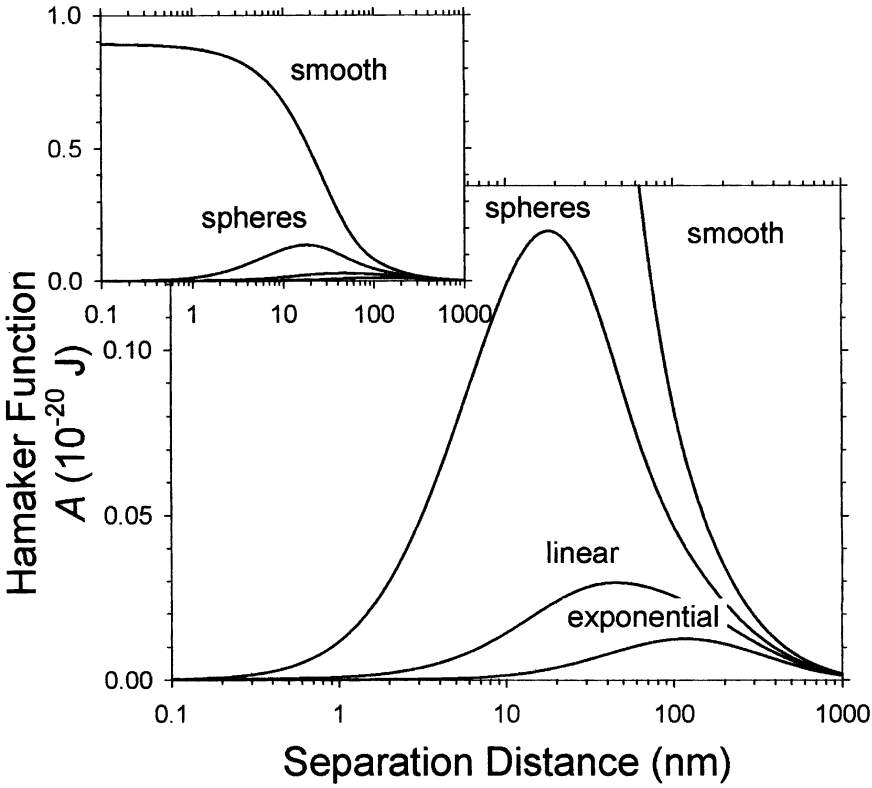

FIGURE 10 Effect of volume fraction profile on the Hamaker function for two polystyrene half spaces separated by water. The volume fraction profiles used were linear, exponential, and the profile for spheres adsorbed on the surface (see Figure 8). The roughness layer thickness was 50 nm for all three cases. For comparison, the interaction between smooth surfaces is also shown. In the insert the ordinate scale has been compressed to show the total variation in the Hamaker function for smooth surfaces.

halfspace correspond to those of the material within a few separation distances of the outer edge of the coating (recall the discussion of Figure 7). As those properties become more water-like, the interaction becomes weaker. In particular, the coating whose volume fraction of water approaches unity at the outer edge appears to have zero attraction at contact of the outer edge (actually, the Hamaker function is not quite zero at contact). For near contact of two such coatings the interaction is like that for two half spaces of water, separated by water: zero attraction.

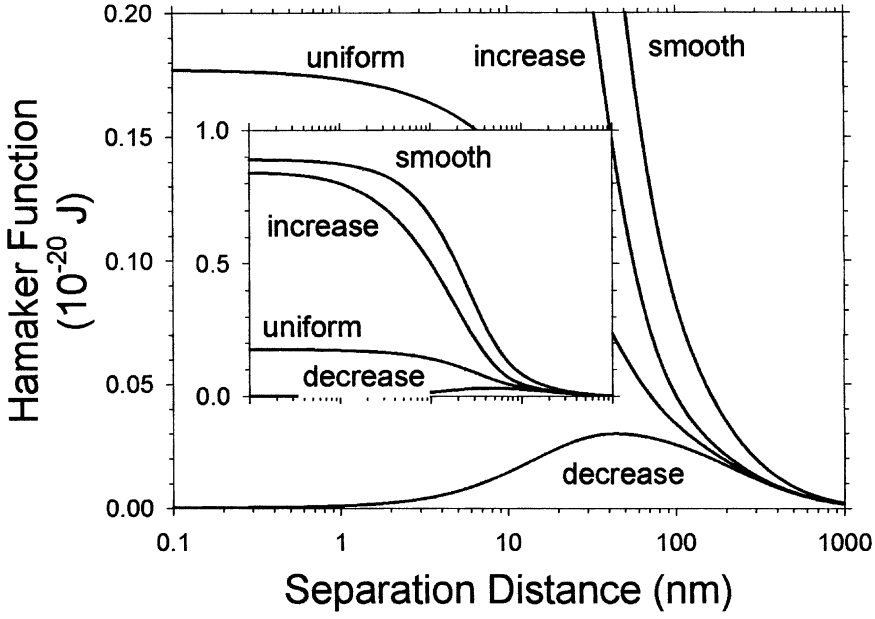

FIGURE 11 Effect of the distribution in volume fraction on the Hamaker function, $A_{132}(L)$, for two polystyrene parallel half spaces, keeping the average volume fraction at 50%. The volume fraction density profiles all had a linear functional form and a total thickness of 50 nm. For comparison, the interaction between smooth surfaces is also shown. In the insert, the ordinate scale has been compressed to show the total variation in the Hamaker function.

Interaction of a Sphere and a Flat

The interaction energy for a 7-micron diameter sphere above a flat plate is shown in Figure 12. The interaction energy for two spheres or a sphere and a flat (relevant to the TIRM experiments discussed later) was calculated using Deraguin's approximation [36],

$$V(h) = \frac{2\pi a_1 a_2}{(a_1 + a_2)} \int_h^\infty -\frac{A_{132}}{12\pi L^2} dL, \tag{16}$$

where a_1 and a_2 are the radii of the two PS spheres. The reduction in value of the Hamaker function from surface roughness translates into weakening of the attractive energy between a sphere and plate. The above trend also is noted in Table 1 by a comparison of the interaction energy values at contact (defined as $h_c = 0.2\,\text{nm}$). The interaction energy for the rough surface with an exponentially decaying density

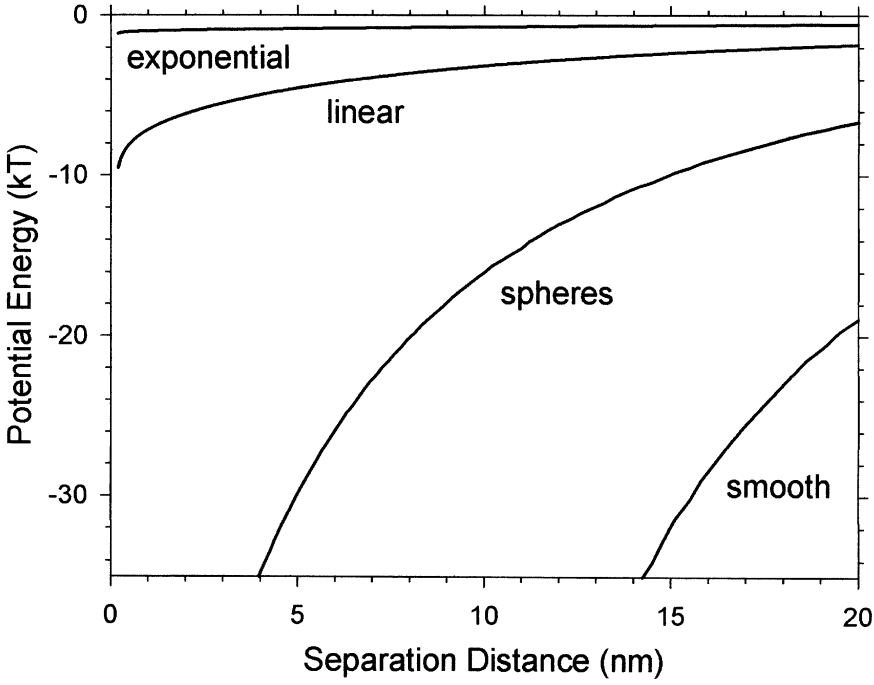

FIGURE 12 The van der Waals interaction energy between a rough plate and a 7-micron sphere generated from the Hamaker functions given in Figure 11 for different volume fraction profiles.

function is four orders of magnitude lower than the interaction for smooth surfaces.

Several qualifications need to be mentioned here regarding Table 1. In particular, these values are not expected to agree quantitatively with any measurements of adhesive energies of PS spheres stuck to a PS plate:

TABLE 1 The van der Waals Attraction Energy at Contact ($h_c = 0.2\,\text{nm}$) Between a 7-micron Diameter Sphere and a Plate

Volume fraction profiles	Energy (k_bT)
Exponential	−1.3
Linear	−11.4
Spheres	−91
Smooth	−12,500

1. Lifshitz's theory for the van der Waals interaction between smooth surfaces diverges at contact owing to the inverse distance dependence in Equation (2). This singularity also arises in Equation (16) with coated surfaces as long as the properties of outermost layer differ from water. To avoid this singularity we used a finite cutoff distance of 0.2 nm [33]. The actual energies vary considerably depending on what is chosen as this cutoff distance.
2. By discretizing the volume fraction profile into 1 nm slices, any calculation of van der Waals interaction below about 5 nm is likely to contain discretization error, at least when the volume fraction tends continuously to zero at the outer edge. To avoid this dicretization error, outer layers need to be thin compared with the separation. Alternatively, the nonretarded theory of Parsegian and Weiss [24] can be employed with a continuous volume fraction profile.
3 Other phenomena not considered here are likely also to become important in the limit of contact, such as deformation of the rough surface as a result of the high compressive stresses.

Despite these qualifications, the observation that surface roughness reduces the magnitude of the van der Waals interaction at contact compared with two smooth surfaces is consistent with adhesion theory and experiments where the strength of adhesion is dominated by local surface asperities and not the overall geometry [37]. The smooth surface for a sphere and plate has one clean contact point (Figure 13a), whereas a rough surface may have several contact points (Figure 13b) and at the same time trapping additional water between the two surfaces. The additional water in the region of contact can be expected to weaken the attraction. The theoretical approach developed using lateral smoothing (Figure 13c) bridges the differences between Figures 13a and 13b. At contact, the van der Waals interaction is dominated by the properties of the outermost coating, which is mostly the intervening medium (water), significantly lowering the interaction energy.

The above argument can be shown by examining the limiting form of the van der Waals interaction for contact. The nonretarded expression for energy [33] without factoring the distance dependence out of the integral is given by

$$E_{132}(L) = \frac{k_b T}{2\pi} {\sum_{n=0}^{\infty}}' \int_0^{\infty} kdk \ln(1 - \Delta_{13}\Delta_{23} e^{-2kL}), \qquad (17)$$

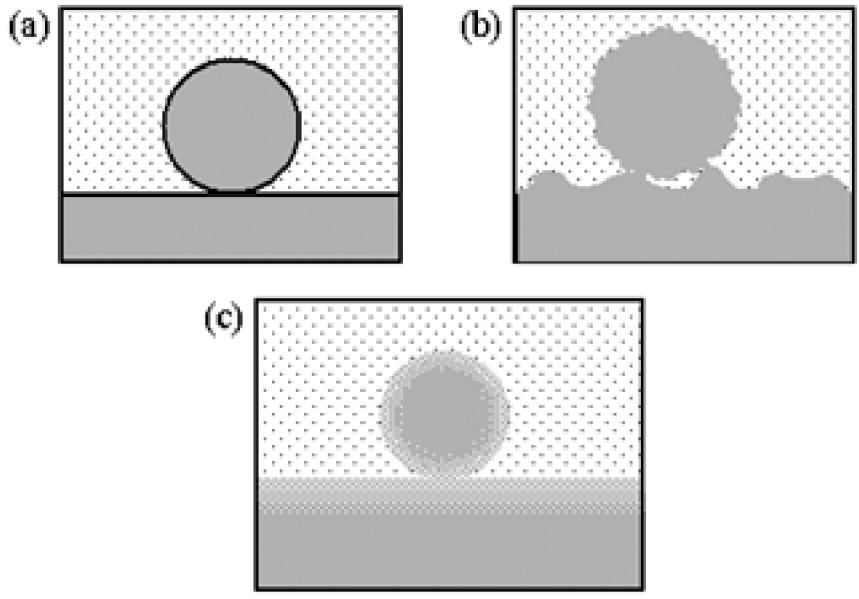

FIGURE 13 (a) A smooth sphere in contact with a smooth plate. (b) A rough sphere in contact with a rough plate where liquid is trapped between the two solid surfaces. (c) A model system of a solid sphere and plate where the solid sphere is covered with a series of coatings changing from mostly solid to mostly liquid and back to solid going from the particle to the flat surface.

where $x = 2kL$. Equation (9) at contact ($L = 0$) leads to

$$\Delta_{31} = \Delta_{3c_N}. \tag{18}$$

The infinite interaction energy comes from the integral over k (or the integral in x in Equation (3)). As $k \to \infty$, the integrand behaves like that for two identical coated halfspaces:

$$k \ln(1 - \Delta_{3c_N}^2), \tag{19}$$

where the nonretarded limit, Δ_{3c_N}, is defined by Equation (1). The above limit is divergent, but as $\varepsilon_{c_N} \to \varepsilon_3$, the rate of the divergence will c_N decrease, thus, the reduction in the interaction at a cutoff distance is observed above. This is consistent with the results of Weiss *et al.* [26] for inhomogeneous coatings on half spaces, where the rate of divergence of the interaction energy at contact was dependent on the how the dielectric permittivity of the coating approached that of the medium outside. In particular, if both the dielectric permittivity and

its derivatives are continuous at the outer edge of the coating, then the interaction energy at contact remains finite.

Limitations of Lateral Smoothing

While the results of lateral smoothing of local asperities are qualitatively consistent with the known weakening of attraction at contact by surface roughness, quantitative applications of the methodology may require separation distances larger than the lateral spacing of the surface features. Mazur and Maradudin were limited to a $L/a > 6$ *via* their derivation (where a is the transverse spacing of surface features), but the results of Mazur and Maradudin apply only to a nonretarded interactions with a Gaussian distribution of surface roughness, and the interaction energy was derived *via* a Taylor series expansion to leading order. The approach developed in this work may also be limited to large L/a values, but it includes retardation, and the expression for the interaction energy is not a truncated series expansion.

Lateral smoothing is less limited in describing a diffuse polymer film. The approach employed in this work is the analogous retarded discrete version of the results of [24, 26, 38] for calculating the nonretarded interactions between surfaces with inhomogeneous dielectric films. The diffuse polymer film is described as a series of coatings with a volume fraction function based on the polymer density from the surfaces. Unlike the application to roughness, the lateral smoothing is now on the molecular level, rather than the scale of features in surface topography, so the mixture is a true solution for which the mixing rule in Equation (13) is well suited.

COMPARISON WITH RETARDED VAN DER WAALS FORCE MEASUREMENTS

We now compare the calculations with measurements of retarded van der Waals attraction obtained with TIRM [38], first for two cases with surface roughness [2] and then for one case having both surface roughness and a physisorbed polymer coating [39].

Glass–PS Rough Surfaces

The interaction energy measured using TIRM between a 6-micron diameter PS particle and a glass slide is shown in Figure 14 [2]. As the NaCl concentration increases, double-layer repulsion becomes screened, exposing the particle to more van der Waals attraction. The roughness of the surfaces was characterized by AFM where the

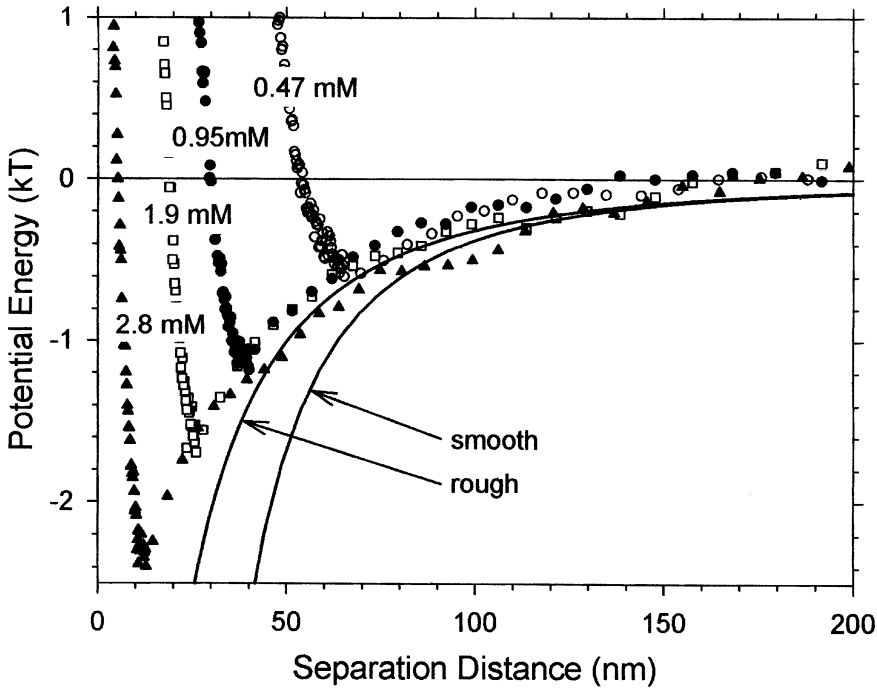

FIGURE 14 Potential energy profiles of the same 6 μm polystyrene particle above a glass plate in aqueous solutions having different NaCl concentrations [2]. The two curves correspond to the fully retarded van der Waals interaction calculated for smooth and rough surfaces.

peak-to-valley roughness was found to be 25 nm for the PS sphere [40]. The glass surface (a BK-7 glass microscope slide, Fisher Scientific, Pittsburgh, PA, USA) was imaged using a Digital Instruments (Santa Barbara, CA, USA) Nanoscope IIIa. The glass surface was cleaned according to the same cleaning procedure used in Bevan and Prieve [2] for glass slides. The AFM image (shown in Figure 15) and volume fraction of glass as a function of depth is given in Figure 6, where the peak-to-valley roughness is 3 nm.

The van der Waals interaction was calculated for rough surfaces using the lateral smoothing method with 2 coatings per nm of roughness. The dielectric spectra for glass was estimated using a Cauchy plot of refractive index in the visible portion of the spectrum [2, 33]. The theoretical curves in Figure 14 only include van der Waals attraction. While the measured attraction is noticeably weaker than predicted between smooth surfaces, the calculations employing lateral smoothing of the roughness result in better agreement, at least at

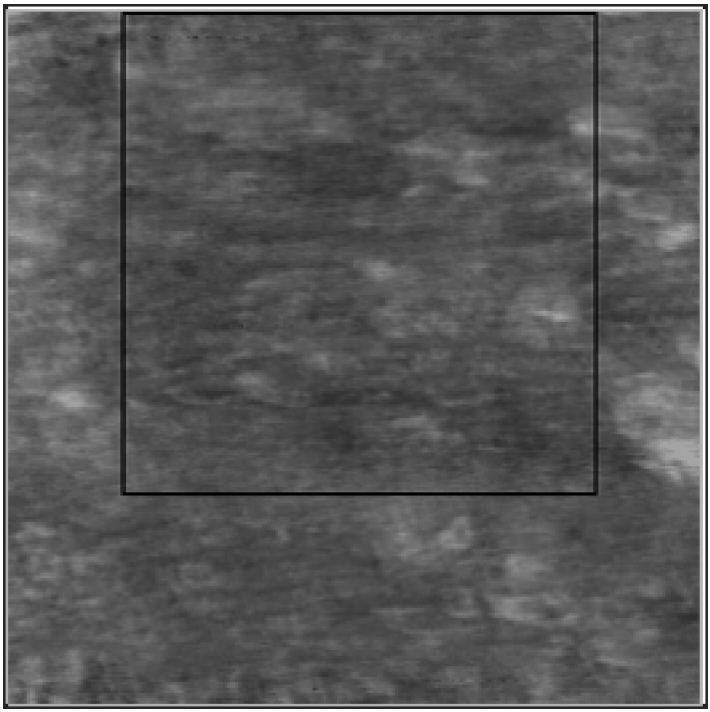

FIGURE 15 Topography of a BK-7 glass slide obtained using AFM. The height scale is 0–3 nm and the scan size is one square micron.

separations above 50 nm. The deviations at smaller separations might be the breakdown in the lateral smoothing approximation as the separation becomes smaller than the lateral spacing of surface features. The strength of attraction would also be overestimated at close separations if the AFM tip was unable to penetrate pores smaller than the tip.

PS–PS Rough Surfaces

Figure 16 shows potential energy profiles measured using TIRM between several 6-micron PS particles and a PS flat in the presence of 1.1 mM sodium dodecyl sulfate [2]. The PS plate is rougher than the glass surface with a peak-to-valley roughness of 10 nm [2], while roughness of the PS sphere was assumed to be the same as in Figure 14. There is some variability in the location of the minimum in the experimental data. This probably arises because the three profiles were taken on three different PS spheres, located over different regions of the PS plate. The variability might result from different

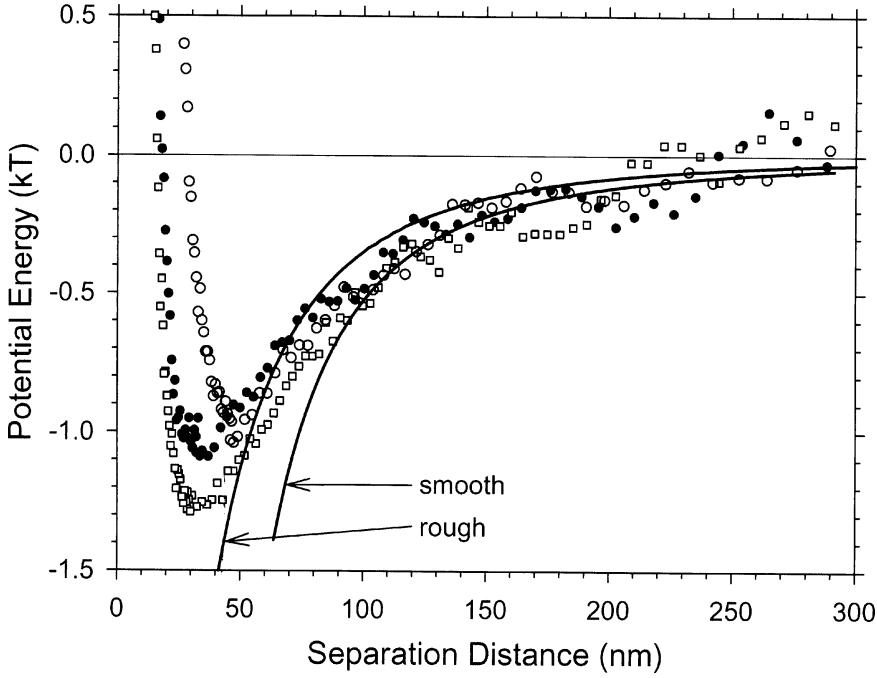

FIGURE 16 Potential energy profiles for three different 6-micron diameter PS particles above a PS flat in 1.1 mM SDS measured with TIRM [2]. The two theoretical curves correspond to the fully retarded van der Waals interaction calculated for smooth and rough surfaces.

charge densities on the three spheres or local variations in the charge density on the plate. The two theoretical curves are for smooth and rough surfaces. As in Figure 14, accounting for roughness in the calculations weakens the van der Waals attraction to about what is measured. Given that there are no adjustable parameters in the model, the improved agreement between theory and experiment in both Figures 14 and 16 is quite remarkable.

Diffuse Polymer Films on Rough Surfaces

Bevan and Prieve [39] used TIRM to measure van der Waals attraction between a 6-micron PS particle and a PS plate when the particle was levitated by steric repulsion between physisorbed layers of F108 Pluronic (BASF, Mt. Olive, NJ, USA) on each surface. Comparing van der Waals attraction between Pluronic-coated surfaces with that between bare surfaces at the same separation between the PS

substrates, they found that the addition of the Pluronic strengthed the van der Waals attraction at long range while causing steric repulsion at short range. Now we will attempt to predict that strengthing by modeling the adsorbed Pluronic layer as a diffuse film on top of a rough surface.

F-108 Pluronic® is a tri-block copolymer of polyethylene oxide (PEO) and polypropylene oxide (PPO) blocks in the form of PEO-PPO-PEO with a molecular weight of 14,000 (for more information on the material properties see Bevan and Scales [41]). The adsorbed polymer forms a diffuse brush on each surface such that the polymer density function decays to zero at approximately 15 nm from the PS surface [39, 42] (see Bevan and Scales [41]). The polymer density function for the Pluronic used in the TIRM measurements is not available, but neutron scattering data for a similar block copolymer was used in the roughness calculations [42]. Tracking the volume fraction of a diffuse polymer film adsorbed on a rough surface poses a complex geometrical accounting of the surface as shown in Figure 17, a schematic of a two-dimensional cross section of an AFM image of a PS surface. In each horizontal layer, there are a water volume fraction, a PS volume fraction, and a Pluronic volume fraction, but the Pluronic density is decaying normal to the interface, resulting in a gradient of polymer volume fractions being sampled in the horizontal coating. Cross sections from a two-dimensional grid on the PS topography image were used to construct the volume fraction functions. For each cross

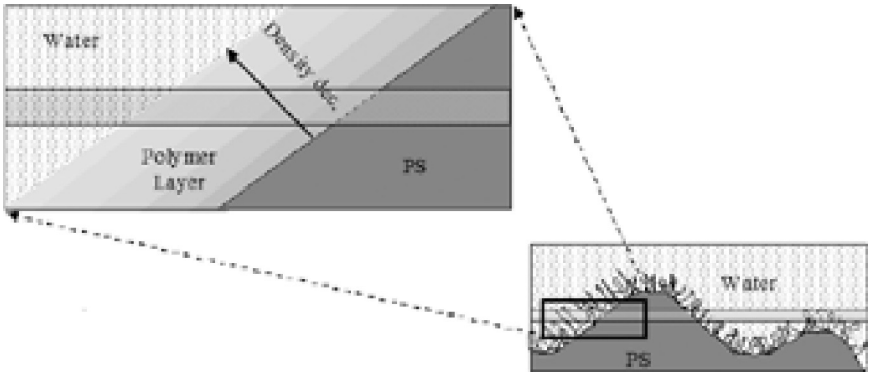

FIGURE 17 A schematic of a two-dimensional cross section of a PS AFM image where a 15 nm polymer film has been added. The horizontal coating is used in the lateral smoothing method, and the individual volume fraction of the PS, water, and adsorbed polymer are used to determine the average material properties.

section, a 15 nm polymer coating was added, where the polymer density decayed normal to the surface (which is not the direction normal to the underlying smooth substrate). The polymer density function was sectioned into 30 coatings and the individual volume fractions of the polymer film were tracked as a function of height from the surface with the volume fraction of PS assigned using the same technique as in the surface roughness case above. The results of each cross-sectional analysis were compiled to construct the volume fraction functions for the surface. The high salt concentrations of the TIRM data completely screen the $n = 0$ term in the van der Waals expressions, but for completeness we derived an expression for electrolyte in the multilayer Hamaker function form in Equations (3) and (10). The amount of screening from electrolyte in each coating was based on the fraction of water (discussed in detail in Appendix A).

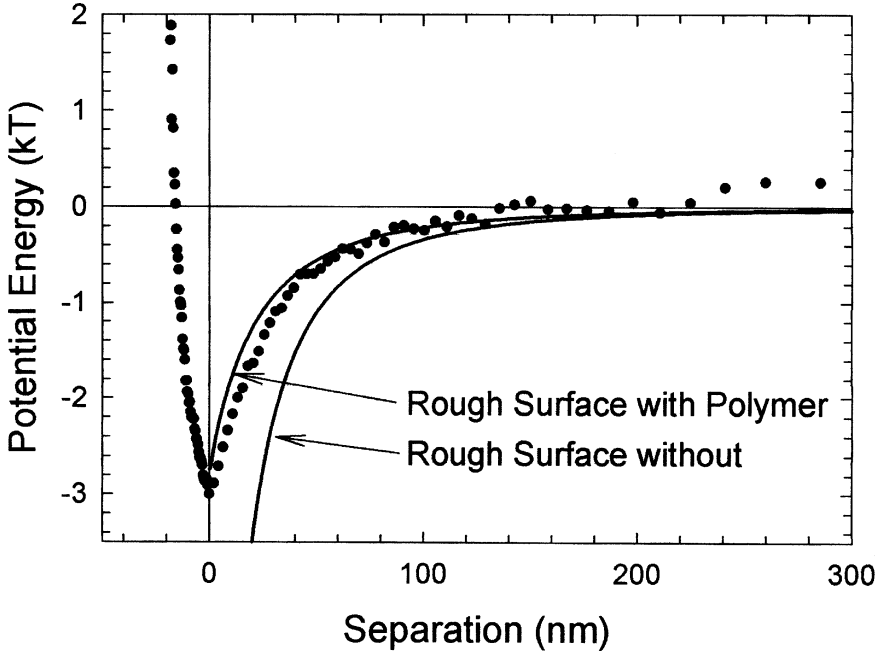

FIGURE 18 The interaction energy of a 6.3-micron PS particle above a PS flat surface with diffuse polymer films adsorbed on each surface in the presence of 400 mM potassium chloride measured with TIRM [39]. The two theoretical curves correspond to the fully retarded van der Waals interaction energy for this system for rough surfaces according to Figure 16, where the solid curve also accounts for the polymer films.

First, we predicted the attraction between two rough surfaces in the absence of polymer (see Figure 18). Once again, no attempt was made to predict the repulsive interaction. Figure 18 also shows the interaction energy measured between a PS particle and a PS plate with F108 Pluronic adsorbed on each surface, in the presence of a high concentration of a binary electrolyte [39]. Zero separation distance corresponds to contact of the outer edges of the two Pluronic layers, or 30 nm separation between the outer edge of the rough PS substrates. Due to the high salt concentration screening the electrostatic forces, the only significant colloidal forces are the long-range attraction from van der Waals forces and the short-range steric repulsion arising from overlap of the polymer films.

Modeling the van der Waals force in this system adds another level of complexity because there is now an adsorbed layer on a rough surface. The result is good agreement between the theoretical calculation and the experimental results in Figure 18 when the effect of the polymer film is taken into account.

IMPORTANCE OF REFERENCE FRAME

When describing the effect of surface roughness or adsorbed polymer on van der Waals forces, the distance used for comparison is crucial. For example, you could compare results defining contact of the outermost surfaces as zero separation or you could define the (hypothetical) contact between the polystyrene substrates as zero. The results in Figures 14 and 16 indicate that the effect of surface roughness is to *weaken* the magnitude of the van der Waals interaction compared with smooth surfaces. This conclusion is based on a reference frame in which the separation distance is measured from contact of the outermost edges of the two interacting surfaces when roughness is added to the surface. On the other hand, if separation between rough surfaces is defined as the distance between the pure PS substrates, the addition of roughness would appear to *strengthen* attraction compared with smooth surfaces.

Contact of the outermost asperities is the natural choice as the definition for zero separation in TIRM experiments because separation distance is obtained by comparing the intensity of a levitated particle with the intensity of a stuck particle (where sticking is caused by salting out double-layer repulsion). There might be some squashing of the largest asperities by strong attraction, but for most hard materials this is more likely to be negligible than complete compression of all of the asperities.

Like roughness, the adsorption of soluble polymer films will also decrease the van der Waals interaction if we define contact of outermost edges of the polymer layers as the zero of separation distance. Then the addition of the diffuse polymer film acts, as a first approximation, to increase the separation between the PS substrates (see Figure 18) and to weaken van der Waals attaction. On the other hand, if instead we define contact of the PS substrates as the zero of separation in both cases, then the adsorption of the diffuse polymer coating of thickness l on each surface at a fixed separation distance greater than $2l$, the main effect is to add material having properties slightly different from water (the intervening medium). Because the soluble polymer has a nonzero Δ relative to water, the two polymer layers will attract one another, adding to the attraction between the PS substrates.

REFERENCES

[1] Suresh, L. and Walz, J. Y. *J. Colloid Interface Sci.* **196**, 177–190 (1997).
[2] Bevan, M. A. and Prieve, D. C. *Langmuir* **15**, 7925–7936 (1999).
[3] Tohver, V., Chan, A., Sakurada, O., and Lewis, J. A. *Langmuir* **17**, 8414–8421 (2001).
[4] Dzyaloshinskii, I. E., Lifshitz, E. M., and Pitaevskii, L. P. *Adv. Phys.* **10**, 165–209 (1961).
[5] Lifshitz, E. M., *Sov. Phys. JETP* **2**, 73–83 (1956).
[6] Ninham, B. W. and Parsegian, V. A. *J. Chem. Phys.* **52**, 4578–4587 (1970).
[7] Nir, S., Rein, R., and Weiss, L. *J. Theor. Biol.* **34**, 135–153 (1972).
[8] Gingell, D. and Parsegian, V. A. *J. Colloid Interface Sci.* **44**, 456–463 (1973).
[9] Gingell, D. and Parsegian, V. A. *J. Theor. Biol.* **36**, 41–52 (1972).
[10] Dagastine, R. R., Prieve, D. C., and White, L. R. *J. Colloid Interface Sci.* **249**, 78–83 (2002).
[11] Dagastine, R. R., Prieve, D. C., and White, L. R. *J. Colloid Interface Sci.* **231**, 351–358 (2000).
[12] Hayashi, H., Watanabe, N., Udagawa, Y., and Kao, C. C. *J. Chem. Phys.* **108**, 823–825 (1998).
[13] Parsegian, V. A. and Ninham, B. W. *J. Theor. Bio.* **38**, 101–109 (1973).
[14] Herman, M. C. and Papadopoulos, K. D. *J. Colloid Interface Sci.* **136**, 385–392 (1990).
[15] Herman, M. C. and Papadopoulos, K. D. *J. Colloid Interface Sci.* **142**, 331–342 (1991).
[16] Sun, N. and Walz, J. Y. *J. Colloid Interface Sci.* **234**, 90–105 (2001).
[17] Walz, J. Y., Suresh, L., and Piech, M. *J. Nanopart. Res.* **1**, 99–113 (1999).
[18] Suresh, L. and Walz, J. Y. *J. Colloid Interface Sci.* **183**, 199–213 (1996).
[19] Maradudin, A. A. and Mazur, P. *Phys. Rev. B: Condens. Matter* **15**, 1677–1686 (1980).
[20] Mazur, P. and Maradudin, A. A. *Phys. Rev. B: Condens. Matter* **23**, 695–705 (1981).
[21] van Kampen, N. G., Nijboer, B. R. A., and Schram, K. *Phys. Lett.* **26A**, 307–308 (1968).
[22] Czarnecki, J. and Dabros, T. *J. Colloid Interface Sci.* **78**, 25–30 (1980).
[23] Czarnecki, J. and Ichenskii, V. I. *J. Colloid Interface Sci.* **98**, 590–591 (1984).

[24] Parsegian, V. A. and Weiss, G. H. *J. Colloid Interface Sci.* **40**, 35–41 (1972).
[25] Vold, M. J. *J. Colloid Interface Sci.* **16**, 1–12 (1961).
[26] Weiss, G. H., Kiefer, J. E., and Parsegian, V. A. *J. Colloid Interface Sci.* **45**, 615–625 (1973).
[27] Kiefer, J. E., Parsegian, V. A., and Weiss, G. H. *J. Colloid Interface Sci.* **51**, 543–546 (1975).
[28] Prieve, D. C. and Russel, W. B. *J. Colloid Interface Sci.* **125**, 1–13 (1988).
[29] Ninham, B. W. and Parsegian, V. A. *J. Chem. Phys.* **53**, 3398–3402 (1970).
[30] Ninham, B. W. and Parsegian, V. A. *J. Chem. Phys.* **52**, 4578–4587 (1970).
[31] Langbein, D. *J. Adhes.* **3**, 213–235 (1972).
[32] Ninham, B. W. and Parsegian, V. A. *Biophys. J.* **10**, 646–663 (1970).
[33] Hough, D. B. and White, L. R. *Adv. Coll. Inter. Sci.* **14**, 3–41 (1980).
[34] Born, M. and Wolf, E. *Principles of Optics*, 5th ed. (Pergamon, Reading, MA, 1975).
[35] Levy, R. A. *Principles of Solid State Physics* (Academic Press, New York, 1968).
[36] Hunter, R. J. *Foundations of Colloid Science* (Clarendon Press, Oxford, 1986).
[37] Israelachvili, J. N. *Intermolecular and Surface Forces* (Academic Press, New York, 1992).
[38] Parsegian, V. A. and Weiss, G. H. *J. Adhes.* **3**, 259–267 (1972).
[39] Bevan, M. A. and Prieve, D. C. *Langmuir* **16**, 9274–9281 (2000).
[40] Considine, R. F., Hayes, R. A., and Horn, R. G. *Langmuir* **15**, 1657–1659 (1999).
[41] Bevan, M. A. and Scales, P. J. *Langmuir* **18**, 1474–1484 (2002).
[42] Fleer, G. J., Stuart, M. A. C., Scheutjens, J. M. H. M., Cosgrove, T., and Vincent, B. *Polymers at Interfaces* (Chapman and Hall, New York, 1993).
[43] Mahanty, J. and Ninham, B. W. *Dispersion Forces* (Academic Press, London, 1976).
[44] Barouch, E., Perram, J. W., and Smith, E. R. *Proc. Roy. Soc. London, Ser. A* **334**, 59–70 (1973).

APPENDIX: EFFECT OF ELECTROLYTE

The Effect of Electrolyte without Coatings

Following van Kampen *et al.* [21], in the absence of free charges the potential satisfies Laplace's equation,

$$\nabla^2\phi(\mathbf{r}) = 0, \tag{20}$$

where $\mathbf{r}$ is the position vector. At the boundary, ϕ and $\varepsilon(\omega)\, d\phi/dz$ are continuous, where z is the distance normal to the interface. In the presence of free charges, the concentration of charge is coupled with potential according to

$$\nabla^2\phi(\mathbf{r}) = -\frac{\rho(\mathbf{r})}{\varepsilon(\omega)} = -\kappa^2\phi(\mathbf{r}), \tag{21}$$

where ρ is the local density of charge and κ^{-1} is the Debye length,

$$\kappa = \left(\frac{\sum_i n_i e^2 z_i^2}{\varepsilon\varepsilon_o k_b T}\right)^{\frac{1}{2}}. \tag{22}$$

The presence of charge in the intervening medium causes a screening of the zero frequency term. The derivation for the $n = 0$ term in Equation (3) with electrolyte begins with Equation (21) and ends with [43]

$$A_{132}(L) = -\frac{3}{4}k_bT\int_0^\infty x\ln[1-\Delta_{13}\Delta_{23}e^{-s}]dx, \tag{23}$$

$$\Delta_{j3} = \frac{\varepsilon_j x - \varepsilon_3 s}{\varepsilon_j x + \varepsilon_3 s} \quad s^2 = x^2 + 4(\kappa L)^2,$$

where z_i is the charge on the ith species, ε is the dielectric constant, ε_o is free space permittivity, e is the charge on an electron, and n_i is the number density of each ion species.

The Effect of Electrolyte with Coatings

We apply the approach outlined in Mahanty and Ninham [43] and Barouch *et al.* [44] for the case with multiple coatings with charge in each coating. For a single coating, the analog of Equation (5) is

$$\Delta_{31}(b) = \frac{\Delta_{34} + \Delta_{41}e^{-(b\beta_4/L)}}{1 + \Delta_{34}\Delta_{41}e^{-(b\beta_4/L)}}, \tag{24}$$

where

$$\beta_i^2 = x^2 + 4(\kappa_i L)^2, \tag{25}$$

where κ_j is the Debye length for each coating, or κ for medium 3. To assign a Debye length to each layer would require knowledge of how the ion concentrations vary with position. This requires a detailed description of rough surface and a numerical solution to the Poisson-Boltzmann equation [16]. We assume that the screening in a coating is determined by the ions in the aqueous fraction and that the solid fraction does not contribute to the screening (neglecting surface charge). Furthermore, we neglect local variations in ion concentration from surface roughness and assume the ion concentration is based on the bulk Debye length. Thus, we set the coating Debye length to the product of the Debye length for smooth surfaces with the aqueous volume fraction for each coating.

Neglecting local changes in ion concentration from surface roughness is reasonable due to the somewhat insensitive nature of screening

to small changes in electrolyte concentration. To illustrate this point, one can examine the form of a common scaling factor to account for screening in the static term between two smooth half spaces in the presence of electrolyte given by [28]

$$(1 + \kappa L)\exp(-2\kappa L), \tag{26}$$

where for binary electrolytes a hundredfold change in bulk concentration (*e.g.*, 0.1 mM to 10 mM) leads to only a tripling of the effects of screening. The above approach can be generalized to any number of coatings in analogous manner to Equation (9), such that

$$\Delta_{31}(c_1, c_2, ..., c_N) = \frac{\Delta_{3N} + \Delta_{N1}(c_1, c_2, ..., c_{N-1})e^{-(c_N\beta_N/L)}}{1 + \Delta_{3N}\Delta_{N1}(c_1, c_2, ..., c_{N-1})e^{-(c_N\beta_N/L)}} \tag{27}$$

is valid, where β_N is defined by Equation (25).